Cylindrical Hall thrusters with permanent magnets

Yevgeny Raitses,[a] Enrique Merino, and Nathaniel J. Fisch
Princeton Plasma Physics Laboratory, Princeton, New Jersey 08543, USA

(Received 12 June 2010; accepted 13 September 2010; published online 10 November 2010)

The use of permanent magnets instead of electromagnet coils for low power Hall thrusters can offer a significant reduction in both the total electric power consumption and the thruster mass. Two permanent magnet versions of the miniaturized cylindrical Hall thruster (CHT) of different overall dimensions were operated in the power range of 50–300 W. The discharge and plasma plume measurements revealed that the CHT thrusters with permanent magnets and electromagnet coils operate rather differently. In particular, the angular ion current density distribution from the permanent magnet thrusters has an unusual halo shape, with a majority of high energy ions flowing at large angles with respect to the thruster centerline. Differences in the magnetic field topology outside the thruster channel and in the vicinity of the channel exit are likely responsible for the differences in the plume characteristics measured for the CHTs with electromagnets and permanent magnets. It is shown that the presence of the reversing-direction or cusp-type magnetic field configuration inside the thruster channel without a strong axial magnetic field outside the thruster channel does not lead to the halo plasma plume from the CHT. © *2010 American Institute of Physics*. [doi:10.1063/1.3499694]

I. INTRODUCTION

The principle of operation of the cylindrical Hall thruster (CHT) (Ref. 1) is based on a closed E × B electron drift and electrostatic acceleration of nonmagnetized ions in quasineutral plasma in a hybrid magnetoelectrostatic trap.[2] The CHT features a reduced surface-to-volume ratio in comparison to a typical annular Hall thrusters [so-called stationary plasma thruster or SPT (Ref. 3)], making it potentially less subject to channel wall erosion by ion-induced sputtering, and more attractive for scaling down to operate at low power. A more detailed comparison of the CHT with other types of Hall thrusters, including SPTs and end-Hall thruster (sometimes called gridless ion source[4]) is given in Ref. 5.

The magnetic field configuration of the CHT can be cusp-type and magnetic mirror-type.[1] Comprehensive studies of the CHT with electromagnet coils are reported elsewhere.[1,2] It was found that for the miniaturized 100–200 W class CHTs (Fig. 1), the optimal magnetic field configuration is an enhanced mirror-type (the so-called direct configuration with the co-direct currents in both electromagnet coils).[6] The highest performance parameters of this thruster were achieved when the maximum magnetic field at the mirror was ~1.5–2 kGauss.[7] In these regimes, the electromagnet coils consumed 50–100 W. For the low power thruster, this additional power consumption reduces drastically the overall thruster efficiency. Therefore, the use of permanent magnets instead of electromagnet coils appears to be a natural choice for the low power CHT. In addition to the reduction in the total electric power consumption, the use of permanent magnets makes the thruster much lighter than the thruster with electromagnet coils. The use of permanent magnets would be required for implementation of the smallest possible Hall thruster scaled down to operate at the lowest allowable power. In this paper, we describe results of discharge and plume measurements for two miniaturized versions of the CHT with permanent magnets (CHTpm): 1.5 cm outer channel diameter CHTpm and 2.6 cm outer channel diameter CHTpm. These results are compared with the discharge and plume characteristics of the low power CHT thrusters (2.6 cm diameter and 3 cm diameter versions) with electromagnet coils, which were comprehensively studied in previous works.[2,5–8]

II. DESIGN CONSIDERATIONS

A typical CHT (Fig. 1) consists of a cylindrical ceramic channel, a ring-shaped anode, which serves also as a gas distributor, a magnetic core made from a low carbon steel, and electromagnet coils or permanent magnets.[1,8,9] The channel can be with or without a short annular part [Figs. 1(a) and 1(b), respectively].[9] which serves to maintain a high ionization of the propellant gas.[1] Although performances of the CHTs with and without annular part (so-called the fully cylindrical Hall thruster or FCHT) are comparable,[10,11] the absence of the annular channel part adds more simplicity to the thruster design. Moreover, probably because of a relatively strong magnetic field oblique to the anode in the annular part, the CHT discharge cannot be initiated without zeroing the coils current or using an auxiliary discharge between the cathode and an additional intermediate electrode placed inside the channel.[12] This is not the case for the thruster of the fully cylindrical configuration.[10] In this configuration, the thruster discharge can be initiated in the presence of a strong magnetic field. There is no a clear understanding of these differences in the discharge initiation between different thruster configurations. Nevertheless, this feature of the FCHT makes this configuration particularly attractive for the implementation of the thruster with permanent magnets.

[a]Electronic mail: yraitses@pppl.gov.

 © 2010 American Institute of Physics

Downloaded 09 Dec 2010 to 198.35.9.115. Redistribution subject to AIP license or copyright; see http://jap.aip.org/about/rights_and_permissions

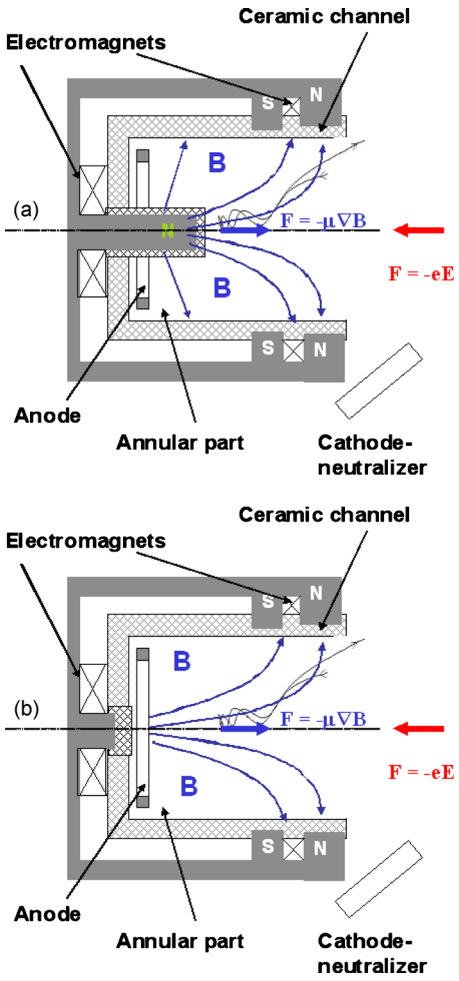

FIG. 1. (Color online) Schematic of a CHT: (a) CHT with a short annular channel and (b) fully cylindrical Hall thruster without a short annular channel (FCHT). Ions are accelerated to the right.

The 1.5 cm and 2.6 cm CHTpm thrusters were designed to operate in the input power range of 50–100 and 100–200 W, respectively. The overall dimensions of the CHTpm thrusters are as follow: for the 2.6 cm CHTpm (Fig. 2), 5.5 cm diameter×3.5 cm length; for the 1.5 cm CHTpm, 3.4 cm diameter×2.4 cm length. For comparison, the 2.6 cm diameter CHT with electromagnet coils[2] is 7.8 cm diameter ×7 cm length. In addition, the 2.6 cm CHT pm is twice lighter (350 g) than its electromagnet counterpart. The thruster mass of the smaller 1.5 cm CHTpm is 110 g. In the described experiments, the 1.5 cm CHTpm has a short (<2 mm) annular part [Fig. 1(a)], while the 2.6 cm CHTpm has a fully cylindrical configuration (FCHTpm) [Fig. 1(b)]. Unlike its larger 2.6 cm diameter counterpart with a short annular channel, the 1.5 cm CHTpm had a reliable discharge initiation and operation.

Each CHTpm thruster uses two axially magnetized permanent magnet rings made from a samarium-cobalt alloy. Like in the thruster with electromagnet coils, these magnet rings are incorporated into the magnetic circuit. Figures 3–6 show results of simulations of the magnetic field produced in the CHT thrusters with electromagnet coils and permanent magnets. In order to implement the direct (enhanced mirror) configuration of the CHT both permanent magnet rings are

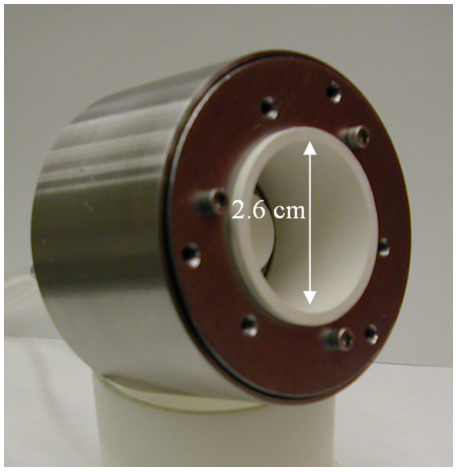

FIG. 2. (Color online) The laboratory 2.6 cm channel diameter CHT thruster with Co–Sm permanent magnets. The overall dimensions of this thruster are 5.5 cm diameter×3.5 cm length. The thruster mass is 350 g. For comparison, the 2.6 CHT with electromagnet coils is 7.8 cm diameter×7 cm length and the thruster mass 700 g.

placed with the same polarity [Fig. 3(a)]. For the cusp configuration [Fig. 3(b)], these rings have an opposite polarity. According to magnetic field simulations and measurements, similarities between the magnetic field distributions produced with permanent magnets (Fig. 3) and electromagnets (Fig. 4) exist only inside the thruster channel. For example, such similarities can be seen for cusp configurations of the 2.6 cm thrusters with permanent magnets and electromagnet coils [Figs. 3(b) and 4(b)]. In the cusp regions of these configurations [between the channel exit and Z≈−0.7 cm, Figs. 3(b) and 4(b)], the magnetic field magnitudes are comparable when the front and back coils currents of the electromagnet CHT are −3.2 A and +3.2 A, respectively [Fig. 5(a)]. These current values are larger than typical coils currents used in

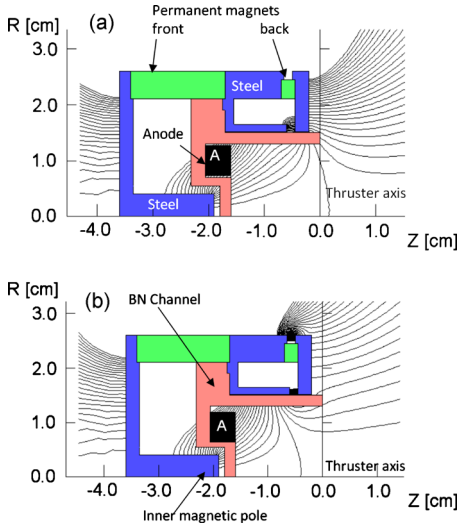

FIG. 3. (Color online) Magnetic field (simulations) in the 2.6 cm diameter fully cylindrical Hall thruster with samarium-cobalt permanent magnets (FCHTpm) and magnetic core made from a low carbon steel: (a) direct (the same axial polarization of both magnets) and b) cusp (opposite polarization); For both these configurations, the maximum magnetic field is ~2–2.5 kGauss at the axis on the back wall of the boron nitride (BN) ceramic channel. Ions are accelerated to the right.

Downloaded 09 Dec 2010 to 198.35.9.115. Redistribution subject to AIP license or copyright; see http://jap.aip.org/about/rights_and_permissions

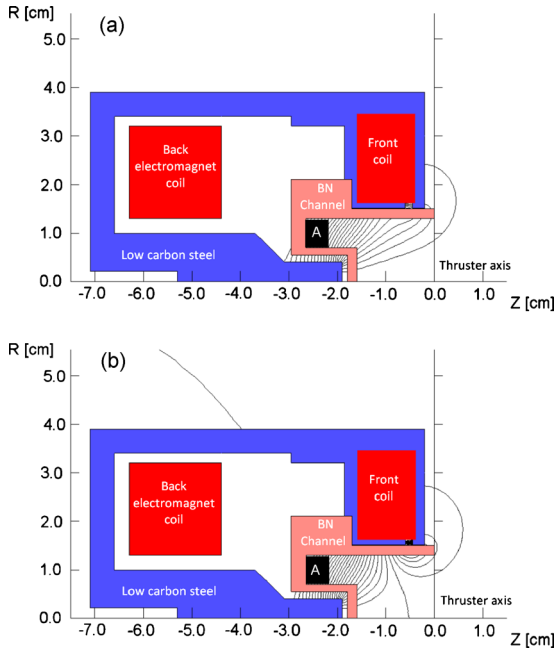

FIG. 4. (Color online) Magnetic field (simulations) in the 2.6 cm diameter cylindrical Hall thruster with a short annular channel and two electromagnet coils: (a) direct (codirected coils currents) and (b) cusp (opposite coils currents); All dimensions are in given in centimeters. For both configurations, the maximum magnetic field is ~1.5–2 kGauss at the axis on the back wall of the BN ceramic channel. Ions are accelerated to the right.

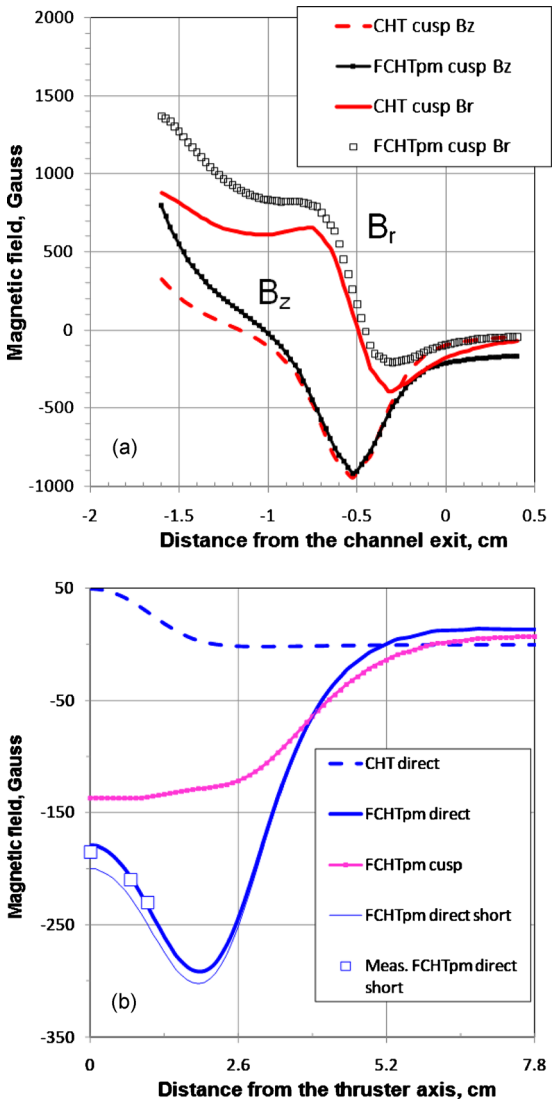

FIG. 5. (Color online) The magnetic field (simulations) for the 2.6 cm channel diameter CHT with electromagnet coils and permanent magnets shown in Figs. 3 and 4: (a) For the cusp configurations shown in Figs. 3(b) and 4(b), axial (Bz) and radial (Bz) components along the outer wall (inside the channel, Z<0). (b) Simulations and measurements of Bz at the distance of 1 cm from the thruster exit. The measured data (using commercial Hall sensor and Gaussmeter) is shown for the 2.6 cm FCHTpm with a 0.5 cm shorter inner pole. The length of the inner pole is shown to have a small effect on the magnetic field outside the thruster channel.

our previous studies (usually, between +/−1 A and +/−2 A for the front coil in direct/cusp configurations, and 2 A and 3 A for the back coil).[2,6] Nevertheless, even with these coils currents, the maximum magnetic field in the magnetic mirror near the back wall of the electromagnet CHT(≤2 kGauss) is smaller than the maximum magnetic field in the permanent magnet thrusters (for the FCHTpm thrusters of Fig. 3, 2–2.5 kGauss at the back wall). Furthermore, outside the thruster channel, the magnetic circuit with the permanent magnets produces a different magnetic field topology. In particular, the magnetic field outside the permanent magnet thrusters is much stronger than the magnetic field outside the CHTs with the electromagnet coils [Fig. 5(b)]. Moreover, with the permanent magnet rings of the same polarity, the direct CHTpm has still a cusped configuration with a reversing-direction axial component of the magnetic field near the channel exit (Figs. 3 and 6).

III. EXPERIMENTAL SETUP

The thrusters were operated in the large PPPL Hall thruster facility.[13] Xenon gas was used in all experiments. The background pressure in a 28 m^3 vacuum vessel equipped with cryopumps did not exceed 3 μtorr. A commercial Heatwave 250 model hollow cathode electron source was used as the cathode-neutralizer. The cathode was placed on a motorized X-Y table in order to change its placement with respect to the thruster axis. The magnetic field in the area of the cathode placement variations is shown in Fig. 6. In these experiments, the cathode gas (xenon) flow rate was maintained constant, 2 SCCM (SCCM denotes cubic centimeter per minute at STP). The cathode keeper electrode was used to initiate the main discharge between the cathode and the thruster anode, and to maintain the discharge current. The keeper current was 0.5 A during the thruster operation.

The plasma plume diagnostics used in these experiments included a planar plume probe with guarding ring for measurements of the angular ion flux distribution in the plume,[13] a bidirectional probe for measurements of the direct ion flux from the thruster and the back ion flux from the background plasma[14] and a two-grid retarding potential analyzer (RPA) for measurements of ion energy distribution function (IEDF). All diagnostic tools were suspended on the rotating platform. The distance between the thruster and rotating plume diagnostics was 73 cm through almost all experiments described in this paper. The exception was IEDF measurements for the 1.5 cm CHTpm, in which the distance between the thruster

Downloaded 09 Dec 2010 to 198.35.9.115. Redistribution subject to AIP license or copyright; see http://jap.aip.org/about/rights_and_permissions

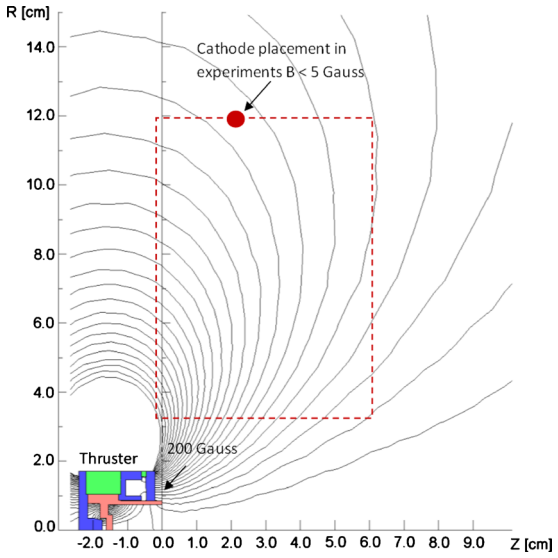

FIG. 6. (Color online) Magnetic field (simulations) for the 1.5 cm CHTpm of the direct configurations and the area of cathode placements (dashed line) explored in these experiments. Measured magnitudes of the axial component of the magnetic field are indicated for the key locations. The filled circle indicates the cathode placement used in plume measurements at different discharge voltages and the RPA measurements. Ions are accelerated to the right.

and the RPA was about 37 cm. This is in order to provide larger signal-to-noise measurements for this small low power thruster with a smaller ion flux than its larger counterparts.

The total ion current was estimated by integrating over measured angular ion flux distribution and then corrected for background plasma effects.[13] The latter procedure was conducted by subtracting the integrated back ion flux, which was measured with the bi-directional probe, from the total ion current.[14] The propellant and current utilization efficiencies were estimated as the ratios of the corrected ion flux to the

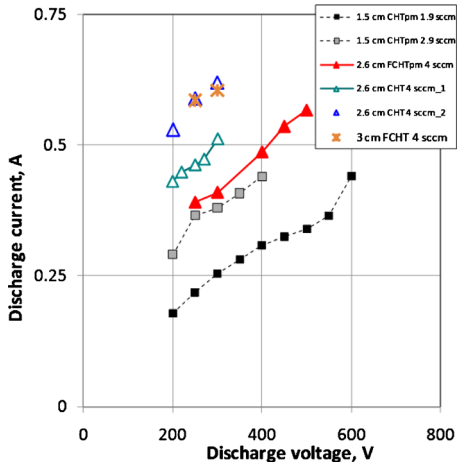

FIG. 7. (Color online) V-I characteristics of the CHT thrusters with permanent magnets and electromagnet coils. The magnetic field is constant. For the 2.6 cm and 3 cm thrusters, the cathode placement was near the channel exit (Ref. 7). For the 1.5 cm CHTpm, the cathode was at the position shown in Fig. 6. For the 2.6 CHT, the second data series was measured at smaller coils currents (magnetic field) than the first data series. The same set of smaller coils currents used for the 3 cm FCHT. The magnetic field in the channel of this fully cylindrical thruster is similar to the 2.6 FCHTpm. The results for the 3 cm FCHT were reported in Ref. 10.

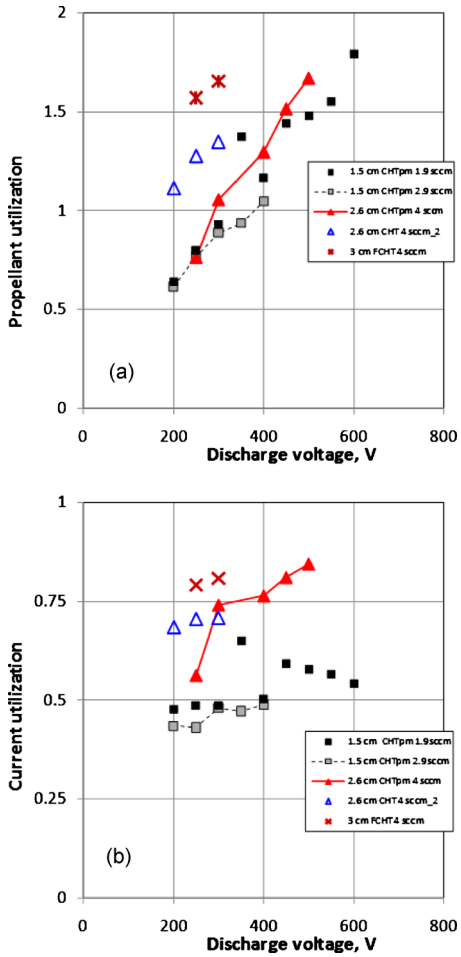

FIG. 8. (Color online) Propellant (a) and current (b) utilization efficiencies for the cylindrical Hall thrusters with electromagnet coils and permanent magnets. The results for the 3 cm FCHT were reported in Ref. 10.

mass flow (in unit of current) and the discharge current, respectively. The plume angle was estimated from the measured angular ion flux distribution for 90% of the total ion current.

IV. EXPERIMENTAL RESULTS AND DISCUSSIONS

Figures 7–10 compare the discharge voltage versus current (V-I) characteristics, plume and ion performance of the permanent magnet and electromagnet CHTs and FCHT. There are notable differences in discharge and ion parameters of the CHT and the CHTpm at discharge voltage below 300–400 V. In these regimes, the thrusters with permanent magnets operate with smaller discharge currents (Fig. 7) and smaller ion currents (can be deduced from Fig. 8) than the thrusters with electromagnet coils. For both thruster types, the increase in the discharge current with the discharge voltage is accompanied with the increase in the propellant utilization [Fig. 8(a)]. Unusually high propellant utilization above 1 [Fig. 8(a)] is typical for CHTs (Refs. 1 and 2) and can be attributed to the presence of a large fraction of multicharged ions, which were previously reported for the miniaturized CHT with electromagnets.[10] For the thrusters with permanent magnets, high ionization regimes occur only at the discharge voltages above 300–400 V. Compared to the

Downloaded 09 Dec 2010 to 198.35.9.115. Redistribution subject to AIP license or copyright; see http://jap.aip.org/about/rights_and_permissions

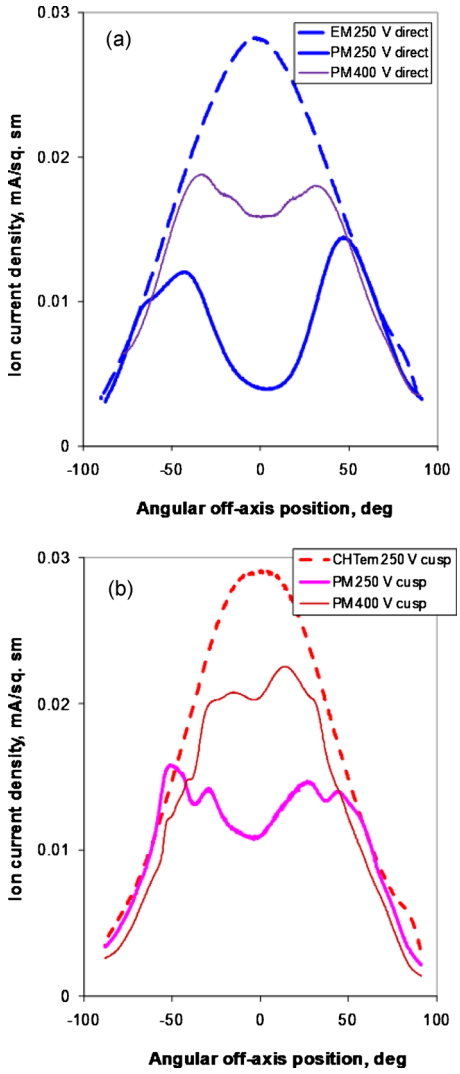

FIG. 9. (Color online) A comparison of angular ion current distributions measured for the 2.6 cm CHT thruster with electromagnetic coils (EM) at xenon gas flow rate of 3.4 SCCM and permanent magnets (PMs) at xenon gas flow rate of 4 SCCM: (a) direct [Figs. 3(a) and 4(a)] The CHT with electromagnets was operated with the front and back coils currents of +2 A and +3 A, respectively, and (b) cusp [Figs. 3(b) and 4(b)]. The CHT with electromagnets was operated with the front and back coils currents of −3.2 A and +3.2 A, respectively.

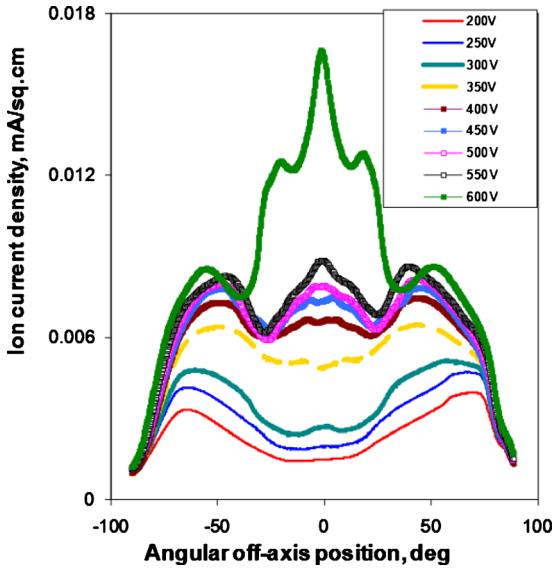

FIG. 10. (Color online) The effect of the discharge voltage on the plume of the 1.5 cm CHTpm thruster. Thruster operating parameters: 250 V, 2 SCCM of xenon flow. The cathode placement in these measurements is shown in Fig. 6.

2.6 cm thrusters with permanent magnets and electromagnets, the 1.5 cm CHTpm operates with the enhanced electron cross-field transport. Unlike for its larger counterparts with permanent magnets and electromagnets, the current utilization efficiency for the 1.5 cm CHTpm remains relatively low with the increase in the discharge voltage [Fig. 9(b)].

The most curious difference between the CHTpm and the CHT thrusters with electromagnet coils is in the shape of their plumes (Figs. 9 and 10). In particular, for the direct configurations, the CHTpm thrusters produce a halo plume with larger ion flux at larger angles with respect to the axis than at the centerline: ~40°–50° for the 2.6 cm FCHTpm (Fig. 9) and ~60°–70° for the 1.5 cm CHTpm (Fig. 10). It was found that this shape is changed, but still exists at different cathode placements.[15] Moreover, the shape of the plume is not strongly affected by changes of the magnetic field in the near anode region of the permanent magnet thrusters. For example, we used two different inner magnet poles, namely, one inner pole was 0.5 cm shorter than the inner pole shown in Fig. 3(a). This difference had a small effect on the magnetic field topology inside the thruster channel and almost no effect on the magnetic field outside the thruster channel [Fig. 5(b) for the cusp configuration]. Moreover, the plume shape was halo and not so different for the thruster operation with these inner magnetic poles. In contrast to this behavior, the central part of the plume shape undergoes a very substantial transformation under variations of the magnetic field topology (Fig. 9 for direct and cusp configurations) and, especially, the discharge voltage (Figs. 9 and 10).

Interestingly, a similar halo shape of the plume was also observed for different versions of the cylindrical geometry thrusters with the permanent magnets, including the diverge-cusped magnetic field thruster (DCF) (Ref. 16) and so-called HEMP thruster.[17,18] However, for the CHTpm thrusters, as the discharge voltage increases, the plume in the vicinity of the centerline appears to be filled with the ion flux (Figs. 9 and 10). For the 1.5 cm CHTpm at high discharge voltages, the plume acquires another unusual shape with multiple peaks of the ion current density (Fig. 10). Unlike the ion flow in the CHT with electromagnets and conventional annular Hall thrusters,[3,19] a majority of energetic ions from the CHTpm flows at larger angles with respect to the thruster axis (Fig. 11). Even at high discharge voltages, when the plume does not have a halo shape, the fraction of energetic ions directed along the centerline is apparently smaller than at larger angles (Fig. 12).

Note that recent thrust measurements demonstrated that for the same discharge voltages and xenon gas flow rates, the 2.6 cm FCHTpm always produces smaller thrust values than its counterparts with electromagnet coils.[20] These thrust measurements were conducted for the direct FCHTpm with the shorter inner pole. In this configuration, the maximum mag-

Downloaded 09 Dec 2010 to 198.35.9.115. Redistribution subject to AIP license or copyright; see http://jap.aip.org/about/rights_and_permissions

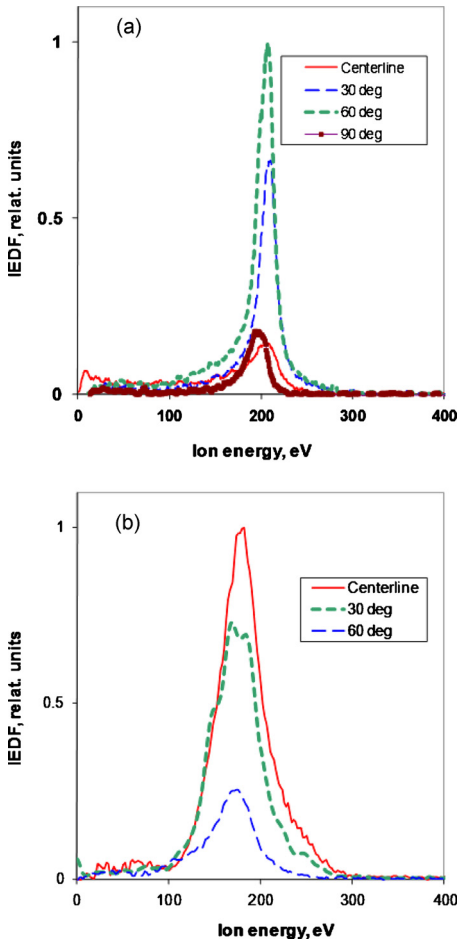

FIG. 11. (Color online) A comparison of the ion energy distribution functions for the CHTs with PMs and electromagnet coils: (a) the 1.5 cm CHTpm at xenon gas flow rate of 2 SCCM and b) the 3 cm CHT with electromagnet coils at xenon gas flow rate of 4 SCCM. The IEDF was measured by the retarding potential analyzer (RPA) placed at the distance of 37 cm from the 1.5 CHTpm and 73 cm from the 2.6 cm CHTem. For the 1.5 cm CHTpm, the cathode placement is shown in Fig. 6. For the 3 cm CHT, the cathode was placed near the channel exit (Ref. 10).

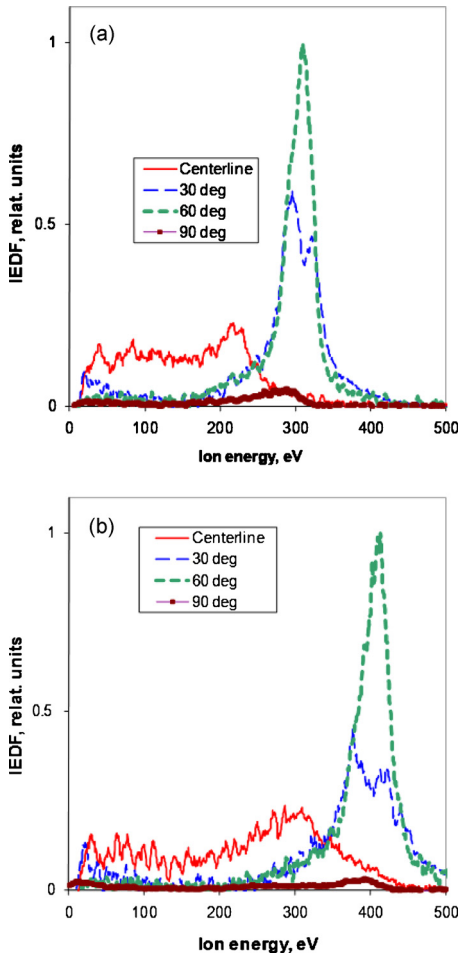

FIG. 12. (Color online) The IEDF for the 1.5 cm CHTpm at the discharge voltage of (a) 350 V and (b) 450 V. The IEDFs were obtained from RPA measurements at the distance of 37 cm from the thruster. The xenon gas flow rate was 2 SCCM. The cathode placement in these experiments is shown in Fig. 6.

netic field at the backwall of the channel was 1 kGauss. This is at least twice smaller than the maximum magnetic field for the FCHTpm configuration of Fig. 3 used in the plume measurements. Nevertheless, the total ion current and the discharge current values were comparable for the FCHTpm with different inner poles. Therefore, a larger plasma divergence and lower propellant utilization of the FCHTpm thrusters [Fig. 8(a)] can explain smaller thrust values measured for the permanent magnet thruster as compared to the CHTs with electromagnets.

We shall now discuss the above results of the plume measurements. For all cathode placements used in the experiments with permanent magnet thrusters, the magnetic field between the cathode and the thruster is relatively strong [Figs. 3 and 5(b)]. Because the electron flow from the cathode to the anode is impeded by this magnetic field outside the thruster, it is possible that a strong electric field is established in this region. If the magnetic field surfaces are equipotential, this electric field should be directed away from the thruster centerline. Heavy xenon ions produced and accelerated inside the thruster channel are nonmagnetized in the plume region ($R_{Li} \gg L$, where R_{Li} is the ion gyroradius and L is the distance between the anode and cathode sides of the acceleration region). In the presence of the radial electric field outside the thruster channel, these ions should be accelerated away from the thruster centerline. For the discharge voltages of below 300 V, the peaks of the ion current density distribution from the direct and cusp configurations of the FCHTpm are at $\theta \approx 40° - 50°$ (Fig. 9) with respect to the thruster centerline. If, for simplicity, we assume that the ions acquire their axial and radial velocities, while they are accelerating inside and outside the channel, respectively, the ratio of the voltage potential drop outside the channel to the voltage potential drop inside the channel is $\Delta\phi_{out}/\Delta\phi_{out} \sim (v_r/v_z)^2 \sim \tan^2(\theta) \approx 0.7-1.4$. This implies that a significant part of the ion acceleration should occur outside the thruster channel. In this respect, another relevant experimental result supporting the existence of significant ion acceleration outside the thruster is well defined peaks of high energy ions on IEDFs measured at the centerline and 90° to the thruster centerline [Fig. 11(a)].

Note that the actual ion acceleration in the CHT with permanent magnets is obviously more complex than described above. Under the assumption of the equipotential

Downloaded 09 Dec 2010 to 198.35.9.115. Redistribution subject to AIP license or copyright; see http://jap.aip.org/about/rights_and_permissions

field lines, one could expect that inside the thruster channel, in addition to the axial velocity directed toward the thruster exit, the ions acquire the radial velocity directed toward the thruster centerline. This is because the magnetic field inside the channel has a strong axial component. The magnetic field lines intersecting the cathode intersect the magnetic circuit or, when the cathode is placed far away from the thruster, the outer wall of the thruster channel in the cusp region near the channel exit. Due to the presence of this cusp region inside the channel, the ions, which are accelerated inside the channel toward the thruster centerline, may continue their acceleration after passing the centerline in the outside electric field. The focusing and defocusing of these ions should depend on details of the magnetic field topology. It is, however, unclear to what extent the magnetic field surfaces are equipotential in the permanent magnet thrusters. In this respect, recent laser induced fluorescence measurements of the CHT with electromagnets revealed that magnetic field surfaces outside this thruster are not equipotential.[21] Keeping in mind that the outside magnetic field topology in the CHT thrusters is very different, the applicability of these results obtained for electromagnet thrusters to the permanent magnet thruster is not so obvious.

Fruchtman and Cohen-Zur[22] predicted that under the assumption of the equipotential magnetic field surfaces and in the absence of the electron pressure gradients, the plume divergence in the $E \times B$ plasma lens is due to the magnetic field curvature and can be approximated as a function of the magnetic field intensity along the ion trajectory, $v_r/v_z \propto (B_i^2 - B_f^2)/(B^2)_{av}$, where B_i and B_f are values of the magnetic field at the beginning and at the end of the ion acceleration, respectively, and $(B^2)_{av}$ is the average value of B^2. They used the paraxial approximation in the description of the ion trajectories in the conventional annular geometry Hall thruster with mainly radial magnetic field. According to Ref. 22, the plume divergence takes place when the ion acceleration starts in the region of a strong magnetic field and ends at the region of a weaker magnetic field, $(B_i^2 - B_f^2) > 0$.

Although the paraxial approximation does not seem to be applicable to complex magnetic field topologies of the CHT thrusters, focusing and defocusing regions likely exist in these thrusters as well. For example, for the cusp configuration of the 2.6 cm FCHTpm, the magnetic field outside the channel is at least two times smaller than for the direct configuration of the same thruster [Fig. 5(b)]. Applying the approach of Ref. 22 one can expect a stronger divergence of the ions, are accelerated toward the centerline and then cross it inside the cusp configuration of this thruster as compared to the direct configuration. Moreover, because the cusp region of the cusp FCHTpm is shifted upstream of the thruster channel as compared to the direct FCHTpm, the radial component of the magnetic field and, presumably, the axial component of the electric field ($E = -v \times B$) are stronger in the cusp configuration. The above differences between the direct and cusp configurations of the permanent magnet thrusters may explain the differences in the angular ion current distribution measured for these thrusters (Fig. 9). This includes

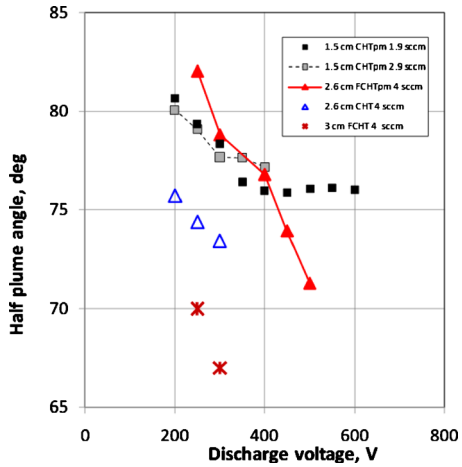

FIG. 13. (Color online) A comparison of the plasma plume divergence measured for cylindrical Hall thrusters of different configurations and geometry with electromagnetic coils and permanent magnets. The results for the 3 cm FCHT were reported in Ref. 10.

the reduced depletion of the ion flow in the vicinity of the centerline of the cusp FCHTM [Fig. 9(b)] as compared to the direct FCHTpm [Fig. 9(a)].

Another important result is that the depletion of the ion flux at the thruster centerline and a halo plume shape cannot be obtained without a strong axial magnetic field outside the thruster channel [Fig. 9(b)]. The plume shape of the cusp CHT with electromagnet coils is almost unaffected by the increase in the magnetic field in the cusp region (increase in the coils currents). Because in this region, the magnetic field intensities are comparable for the permanent magnet and electromagnet thrusters [Fig. 5(a)], a key difference between the cusp FCHTpm [Fig. 3(b)] and the cusp CHT with electromagnet coils [Fig. 4(b)] is a stronger magnetic field outside the permanent magnet thruster [Fig. 5(b), between R = 0 and 4 cm). This result additionally supports a key role of the outside magnetic field in the formation of the plasma flow in the permanent magnet thrusters.

Spatial variations of the ion production inside and outside the channel could also affect the ion trajectories. A combined effect of these variations and ion acceleration inside and outside the channel, as well as their dependence on the discharge voltage, should affect the angular distribution of the ion flow, including its shape and the IEDF. In particular, variations in the ion production along the channel could explain changes of the plume shape with the discharge voltage (Fig. 9) and the presence of multiple peaks in the plume of the 1.5 cm CHTpm (Fig. 10). With respect to the latter, it is interesting to note that there is a correlation between the occurrence of such peaks in the angular ion flux distribution and the saturation of the plume angle at high discharge voltage (Fig. 13). For other CHT thrusters, including electromagnet and permanent magnet versions, the plume tends to become narrower with the discharge voltage. Moreover, for the smaller CHTpm, the IEDF is changed with the discharge voltage so that a broader energy spectrum of ions appears at the centerline and less energetic ions at 90° to the thruster axis. These results may indicate that as the discharge voltage increases the ion production inside the thruster channel in-

Downloaded 09 Dec 2010 to 198.35.9.115. Redistribution subject to AIP license or copyright; see http://jap.aip.org/about/rights_and_permissions

creases. Measurements of the plasma properties inside the thruster and in the near-field plume could help to determine the relevance and the importance of these effects for the permanent magnet thrusters.

Finally, dynamic processes in the thruster discharge, including so-called breathing oscillations (10–14 kHz) of the discharge current and the rotating spoke oscillations (3–4 kHz) which were reported in Ref. 15 might also contribute to the formation of the angular distribution of the ion flow and the IEDF in the permanent magnet thrusters.

V. CONCLUSIONS

Results of plume measurements for different miniaturized cylindrical Hall thrusters with different magnetizing sources suggest that the operation of the thrusters with permanent magnets is different from the thrusters with electromagnet coils. The ion current density distribution in the plume of the permanent magnet CHTs has an unusual halo shape with a majority of energetic ions flowing at large angles of 40°–70° (depending on the magnetic configuration and the thruster channel diameter) with respect to the thruster axis. Apparently, in the thrusters with permanent magnets, the electric field accelerates high energy ions away from the centerline. This is different from all electromagnet versions of the CHT, in which high energy ions are accelerated toward and parallel to the thruster centerline.[21] It is hypothesized that this difference in the ion acceleration between the cylindrical thrusters with electromagnet coils and permanent magnets is, in large part, because of a stronger axial magnetic field outside the permanent magnet thrusters. This magnetic field might alter the plasma potential distribution in a way that a significant portion of the ion acceleration occurs outside the channel by a defocusing radial electric field in this region.

In addition, the presence of the reversing-field magnetic field in the channel of the direct (magnetic mirror topology) and cusp configurations of the permanent magnet thrusters might also contribute to the differences in the plasma plume characteristics especially as compared to the direct configuration of the electromagnet CHT. However, it was demonstrated that the reversing-field configuration without a strong magnetic field outside the thruster channel cannot produce a halo shape of the plasma plume.

Similarities between the magnetic field outside the channel and the plume shape measured in three permanent magnet versions of the cylindrical thruster, including the CHTpm, DCF (Ref. 16) and HEMP,[17,18] suggest that all three thruster types operate in a similar way in which the outside electric and magnetic fields play a critical role in the formation of the plasma jet and, thereby, the thrust generation.

Note that the actual plasma potential distribution and the plasma flow in the permanent magnet thrusters is likely more complex than hypothesized in this paper. For example, critical questions are related to equipotentiality of the magnetic field surfaces in the magnetic field configurations of the CHT,[5,21,23] including its electromagnet and permanent magnet versions. Detailed plasma measurements in these thrusters as well as related theoretical and simulation efforts are required to address these questions.

Finally, it is worth mentioning that despite larger divergence of energetic ions and smaller propellant utilization leading to smaller thrust values, the thruster efficiency of the permanent-magnet thrusters compares favorably with the efficiency of the electromagnet thrusters when the power consumed by the electromagnet coils is taken into account [at the discharge (anode) power of 100–150 W, ~18% compared to ~15.5%, respectively].[20]

ACKNOWLEDGMENTS

The authors wish to thank Dr. Kevin Diamant of the Aerospace Corporation and Dr. Kurt Polzin of NASA Marshall SFC for fruitful discussions. The authors are grateful to Mr. Jean Carlos Gayoso of the PPPL for his assistance with simulations and measurements of the magnetic field. This work was supported by the AFOSR and the U.S. Department of Energy under Contract No. AC02–76CH0–3073.

[1] Y. Raitses and N. J. Fisch, Phys. Plasmas **8**, 2579 (2001).
[2] A. Smirnov, Y. Raitses, and N. J. Fisch, Phys. Plasmas **14**, 057106 (2007).
[3] A. I. Morozov and V. V. Savelyev, in *Review of Plasma Physics*, edited by B. B. Kadomtsev and V. D. Shafranov (Consultants Bureau, New York, 2000), Vol. 21, p. 203.
[4] H. R. Kaufman, R. S. Robinson, and R. I. Seddon, J. Vac. Sci. Technol. A **5**, 2081 (1987).
[5] Y. Raitses, A. Smirnov, and N. J. Fisch, J. Appl. Phys. **104**, 066102 (2008).
[6] A. Smirnov, Y. Raitses, and N. J. Fisch, IEEE Trans. Plasma Sci. **34**, 132 (2006).
[7] A. Smirnov, Y. Raitses, and N. J. Fisch, Phys. Plasmas **11**, 4922 (2004).
[8] A. Smirnov, Y. Raitses, and N. J. Fisch, J. Appl. Phys. **92**, 5673 (2002).
[9] Y. Raitses and N. J. Fisch, "Cylindrical Geometry Hall Thruster," U.S. Patent No. 6,448,721 B2, September 2002; Y. Raitses, N. J. Fisch, K. M. Ertmer, and C. A. Burlingame, Proceedings of the 36th Joint Propulsion Conference, Huntsville, AL, July 2000.
[10] K. D. Diamant, J. E. Pollard, Y. Raitses, and N. J. Fisch, IEEE Trans. Plasma Sci. **38**, 1052 (2010).
[11] A. Shirasaki and H. Tahara, J. Appl. Phys. **101**, 073307 (2007).
[12] Y. Raitses, A. Smirnov, E. Granstedt, and N. J. Fisch, Proceedings of the 43rd AIAA/ASME/SAE/ASEE Joint Propulsion Conference & Exhibit, Cincinnati, OH, July 2007 (AIAA, Reston, VA, 2007), AIAA paper 2007-5204.
[13] Y. Raitses, D. Staack, A. Dunaevsky, L. Dorf, and N. J. Fisch, Proceedings of the 28th International Electric Propulsion Conference, Toulouse, France, March 2003 (ERPS, Cleveland, OH, 2003), IEPC paper 03-0139.
[14] Y. Raitses, T. Moeller, and J. Szabo, Proceedings of the 30th International Electric Propulsion Conference, Florence, Italy, September 2007 (ERPS, Cleveland, OH, 2007), IEPC paper 2007-334.
[15] Y. Raitses, E. Merino, J. B. Parker, and N. J. Fisch, Proceedings of the 45th AIAA/ASME/SAE/ASEE Joint Propulsion Conference & Exhibit, Denver, CO, August 2008 (AIAA, Reston, VA, 2008), AIAA paper 2009-4810.
[16] D. G. Courtney, P. Lozanoy, and M. Martinez-Sanchez, Proceedings of the 44th AIAA/ASME/SAE/ASEE Joint Propulsion Conference & Exhibit, Hartford, July 2008 (AIAA, Reston, VA, 2008), AIAA paper 2008-4631.
[17] N. Koch, H.-P. Harmann, and G. Kornfeld, Proceedings of the 29th International Electric Propulsion Conference, Princeton, NJ, October 2005 (ERPS, Cleveland, OH, 2005), IEPC paper 2005-297.
[18] K. Matyash, R. Schneider, A. Mutzke, O. Kalentev, F. Taccogna, N. Koch, and M. Schirra, IEEE Trans. Plasma Sci. **38**, 2274 (2010).
[19] J. Bareilles, G. J. M. Hagelaar, L. Garrigues, C. Boniface, J.-P. Boeuf, and N. Gascon, Phys. Plasmas **11**, 3035 (2004).
[20] K. A. Polzin, E. S. Sooby, A. C. Kimberlin, Y. Raitses, E. Merino, and N. J. Fisch, Proceedings of the 45th AIAA/ASME/SAE/ASEE Joint

Downloaded 09 Dec 2010 to 198.35.9.115. Redistribution subject to AIP license or copyright; see http://jap.aip.org/about/rights_and_permissions

Propulsion Conference & Exhibit, Denver, CO, August 2009 (AIAA, Reston, VA, 2009), AIAA paper 2009-4812.
[21]R. Spektor, K. D. Diamant, E. J. Beiting, Y. Raitses, and N. J. Fisch, Phys. Plasmas **17**, 093502 (2009).
[22]A. Fruchtman and A. Cohen-Zur, Appl. Phys. Lett. **89**, 111501 (2006).
[23]N. J. Fisch, A. Fetterman, Y. Raitses, A. Fruchtman, and J.-M. Rax, Proceedings of the 44th AIAA Joint Propulsion Conference, Hartford, CT, July 2008 (AIAA, Reston, VA, 2009), AIAA paper 2008-4997.

Downloaded 09 Dec 2010 to 198.35.9.115. Redistribution subject to AIP license or copyright; see http://jap.aip.org/about/rights_and_permissions